INVESTIGATIONS OF THERMAL PARAMETERS ADDRESSED TO A BUILDING SIMULATION MODEL

Christian Brembilla[1], Calude Lacoursiere[2], Mohsen Soleimani-Mohseni[1], Thomas Olofsson[1]
[1]Department of Applied Physics and Electronics, Umeå University, Umeå, Sweden
[2]High Performance Compting Center North (HPC2N), Umeå University, Umeå, Sweden

ABSTRACT

This paper shows the tolerance of thermal parameters addressed to a building simulation model in relation to the local control of the HVAC system. This work is suitable for a modeler that has to set up a building simulation model. The modeler has to know which parameter needs to be considered carefully and vice-versa which does not need deep investigations. Local differential sensitivity analysis of thermal parameters generates the uncertainty bands for the indoor air. The latter operation is repeated with P, PI and PID local control of the heating system. In conclusion, the local control of a room has a deterministic impact on the tolerance of thermal parameters.

INTRODUCTION

Thermal parameters of existing buildings are usually evaluated in the literature by modellers. These parameters are typically addressed to a thermal simulation model to assess the building energy performance and energy conservation measures. The high grade of uncertainty in the evaluation of existing buildings can affect the simulated results. A modeller has to know which parameter must be carefully detected and which instead does not need deep investigations. Several authors document uncertainties in the evaluation of thermal parameters of existing buildings. However, to the knowledge of the writer, only few works argue about the uncertainty bands related to the room temperature. For instance, (Clarke et al. 1993) analyses the variation of room temperature subjected to the perturbation of input parameters. The model is developed in ESP-r environment. The author compares the local with the global sensitivity analysis on input parameters. The latter analysis is developed with Monte Carlo method by varying all the input simultaneously. Uncertainty bands calculated from both analyses do not show significant discrepancies. The uncertainty bands of indoor air are also discussed by Spitz in (Spitz et al. 2012). The author develops a methodology to order the thermal parameters that have the most affect on the indoor temperature. The starting point is the local sensitivity analysis, then the global sensitivity analysis and lastly the uncertainty analysis. Results show the parameter that has most influence on the indoor air which is the capacity of electric heating system, followed by the heat exchanger efficiency and in third position the internal loads. Moreover, the author states that parameters do not affect the indoor temperature could be simplified or sometimes neglected. Heo in (Heoa et al. 2012) shows uncertainty bands of indoor air by means of the use of measured data, highlighting that the indoor air does not have a uniform value in the entire air volume of the room. However, all the previous authors and others agree that the internal loads from free sources and HVAC system mainly influence the indoor air (Silva et al. 2014). Uncertainty bands of indoor temperature has not been yet investigated in relation to the local control of the HVAC system. The local control adjusts the thermal power supplied to the room and consequently it affects on the indoor temperature. The control works with threshold values fulfilling the range of thermal comfort for occupants. The scope of this work is to show how the local control strategy of the room heating system is essential for evaluating the tolerance of thermal parameters. A detailed description of a room equipped with panel radiator is presented. The room is modeled with a hybrid method, combining recorded input parameters with its physical characterization. Differential sensitivity analysis are applied locally to each thermal parameter one at a time, performing the uncertainty bands for indoor air. The tolerance value of each thermal parameter is evaluated by perturbing again each parameter until CV RMSE is fulfilled. Lastly, the local control of the room is switched among P, PI and PID. The tolerance of thermal parameters are provided for each control emphasizing that the modeller should carefully evaluate this factor.

NUMERICAL MODEL OF THE ROOM

This section describes the numerical model of the room used to estimate the tolerance of thermal parameters. At first, a short overview describes advantages and drawbacks of some simulation models employed in the research field. Following the mathematical model of the room is introduced, and last sub-section describes the model thermal parameters.

Choose of simulation model

In literature it is possible to find plenty of energy simulation models for buildings. The major difficulty is to know which model is more suitable for the case studied. The quality of available information and the expected results affect this choice. Usefulness of some energy simulation models for buildings are presented together with advantages and drawbacks for each case

(Swan et al. 2009). Steady state models are used to assess building energy performance and they have the lead to be simple, for this reason, they are implemented in national building codes. Conversely, steady state models does not provide any information about the transient response of the building and its HVAC system (Armstrong et al. 2006). Models that consider the heat stored in elements are often modelled with finite difference methods. Such models analyze the transient thermal behavior of a single zone, walls or the HVAC system components. These models have as drawback to be computationally heavy and time consuming for developing the code. Additionally, a good knowledge of heat transfer mechanism and computer programming are essential conditions by the modeler for developing the simulation. For these reasons, the transfer function became more popular for its simplicity and low computational cost. For example, the commercial software TRNSYS uses z-transformation to transfer the heat through the building envelope (TRNSYS et al. 2012). Other commercial software, as IDA ICE, ESP-r, Energy+…, perform the dynamic simulation of the building and HVAC system given the freedom to vary pre-set parameters of the model. Lumped capacity models simplify the whole building in one thermal capacitance. The apartment is modelled as one single zone at which lighting, occupancy and equipment appear as heat gains in the heat balance. These models are largely used for extrapolating results at regional or national level (Mata et al. 2010, Muratori et al. 2012). Nevertheless, lumped capacity models do not account the effects of thermal mass on indoor temperature. The thermal mass is accountable of store and release heat during the day. It must be underlined that the thermal mass which actively interacts with indoor air is only the first layer in contact with the conditioned space. The thermal mass adjacent with the outside environment does not affect much the indoor air. The thermal insulation positioned between internal and external mass works as a damper of the heat wave. This work introduces the effective thermal mass with the name of active layer. The model presented in this paper considers the mutual effects between active layer and indoor air. The power of the model is its hybrid nature, it is robust in the prediction of thermal performance because its structure can be physically interpreted and input parameters can be identified from available data (Shengwei et al. 2012, Xinhua et al. 2005). Furthermore, simplicity, flexibility and quick analysis are the main strengths of the model. The model presented in the following paragraphs allows the controllability of the HVAC system, extrapolating results to a regional or national level.

Mathematical model

The numerical model of the room consists of two lumped capacitances that represent air volume and active layer (Säppanen et al. 2004). Left side of Figure 1 shows a typical cross section of a room where the active thermal mass is in yellow. Right side of Figure 1 shows the network of the hybrid model made by with resistances and capacitances. The model does not consider the thermal effect due to the furniture.

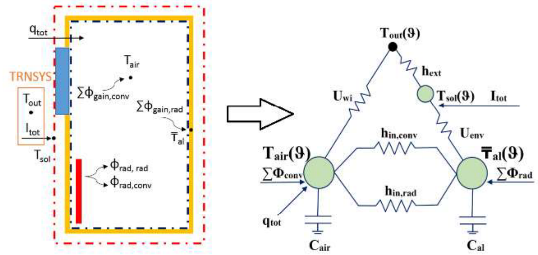

Figure 1 Left side. Cross section of a room. Right side. Resistors and capacitors schema

The mathematical model is a system of two non linear ordinary differential equations with non-homogenous parameters resolved simultaneusly by (1). The equations are coupled by means of the temperature of indoor air and the average temperature of active layer.

$$\begin{cases} C_a \frac{dT_{air}}{d\vartheta} = H_1\cdot\left(\overline{T_{al}}-T_{air}\right) + H_2\cdot\left(T_{out}-T_{air}\right)) + q_{tot}\cdot\left(T_{out}-T_{air}\right) + \sum \emptyset_{i,c.} \\ C_{al}\frac{d\overline{T_{al}}}{d\vartheta} = H_3\cdot\left(T_{air}-\overline{T_{al}}\right) + H_4\cdot\left(T_{sol}-\overline{T_{al}}\right) + \sum \emptyset_{I,rad.} \end{cases} \quad (1)$$

where:

$H_1 = h_{in,c.}\cdot A_{al}$, $H_2 = U_{wi}\cdot A_{wi}$, $H_3 = h_{in,r}\cdot A_{al}$,

$$H_4 = \left(\frac{1}{U_{env.}} - \frac{1}{h_{int,r}} - \frac{1}{h_{ext}}\right)^{-1}\cdot A_{env.}$$

The first equation in (1) is the heat balance of the air volume, which exchanges heat through windows, ventilation, cracks, active thermal mass, and the heat generated by convection from radiators and other sources. The second equation in (1) shows the heat balance of the active layer. In the latter equation the heat is exchanged between indoor, outdoor air, and the radiative heat generated by radiation. It also appears the variable T_{sol} that is the temperature on the external surface facing the outside environment. It is calculated with Equation (2):

$$T_{sol} = T_{out} + \frac{\beta\cdot I_{tot}}{h_{ext}} \quad (2)$$

Walls have set up the adiabatic condition, this means that no heat passes to the neighboring rooms unless the wall facing to outside environment.

Estimate values of the model

The thermal parameters addressed to the simulation model are ranked in Table 1 according to literature parameters (Adamson et al. 2011). Nevertheless, some parameters require further explanations about their physical characterization. The coefficients of heat transfer by convection and radiation for internal surfaces ($h_{in,r}$, $h_{in,c}$) depend on the surface orientation. This model does not make difference about the surface orientation, hence a constant coefficient of $3 Wm^{-2}K^{-1}$ is set for both convection and radiation. The coefficient of heat transfer by convection on the external surface (h_{ext}) is set up at 20 $Wm^{-2}K^{-1}$ considering wind effects (TRNSYS et al. 2012). The ventilation by cracks is 0.1ach and 0.5ach for natural ventilation. The simulation considers two active layers. The first one is regarding the floor, ceiling, internal walls; it is 0.08m thick and it is composed by two materials: brick and plaster. The second is the active layer of the envelope with a thickness of 0.15m composed by brick and plaster. The total capacitance of the active layer is the sum of the single capacitance of each layer.

Table 1 Parameters addressed to the simulation model

Geometric parameters			**General parameters**		
Volume	V	41.6 m^3	Air density	ρ_{air}	1.2 kgm^3
Surface active layer	A_{al}	63.2 m^2	Specific h. cap.	c_{air}	1005 $Jkg^{-1}K^{-1}$
Envelope surface	A_{env}	8.6 m^2	Tot. air change	ach	0.6
Window area	A_{wi}	1.8 m^2	**Parameters calculated**		
Thermal parameters			Ventilation load	q_{tot}	8.37 WK^{-1}
Envelope conductance	U_{env}	0.5	Volume cap.	C_{air}	$5.02\cdot10^4$ JK^{-1}
Window conductance	U_{wi}	1.8	Activ. layer ca.	C_{al}	$5.20\cdot10^6$ JK^{-1}

INPUT PARAMETERS

This section describes the input parameters addressed to the simulation model. In absence of measured data, outdoor temperature and the sun radiation on horizontal surface are read from TRNSYS simulation software. The first sub-section reports about the internal loads profile. The second subsection tells about the thermal power from the panel radiator and lastly the thermal power from sun radiation.

Internal loads

The thermal power from the persons is scheduled according to standard profiles of occupancy with 71W for low activity and 119W for normal activity. During the week the normal activity is between 7 to 8a.m. and 6 to 11p.m. The low activity is between 11p.m. to 7a.m. In the week-ends the high activity is considered from 10a.m. till 1.00p.m. and between 6p.m. and 8p.m. whilst the low activity between midnight and 10a.m. The latent heat from person is not considered in this calculations. Lighting is more complex, since the season affects the total quantity of natural light available in the room. It is simply assumed that lights are always on during winter time according to the high level of occupancy with power of 5 Wm^{-2} (Cengel et al. 2010). Lights are off during the summer time and they work at half power during autumn and spring season. Appliances from computer, television and other electrical devices are accounted as a heat gain of 100W during the evening from 8p.m. till 11p.m. Electrical devices are off during the week-ends. The radiative and convective heat gain from all the free sources is considered in the air volume with the same proportion of 50%. The power from free sources is included in the last term in (1) and the extensive form is presented in Equation (3).

$$\sum\phi_{i,c/r} = \phi_{occ,c/r} + \phi_{light,c/r} + \phi_{app,c/r} + \phi_{rad,c/r} + \phi_{sun,c/r} \quad (3)$$

Modelling the power from panel radiator

The power from panel radiator appears in the room as convection and radiation heat gain. These thermal loads are essential information addressed to the simulation. The demonstration is not rigorous, because the transient behavior of the panel is not implemented in the following calculations. The radiator adds energy to the room instantaneously according to the control strategy adopted. Such radiator operates in a range of temperature supply flow of 30-55ºC, which is not known a priori, but it can be predicted by using the heating curve (Vitotalk et al. 2003). The heating curve correlates the supply temperature with the outside temperature, acting as general controller ensuring that an adequate amount of heat is delivered to the building. For this purpose, a typical heating curve is deducted numerically from technical catalog. The polynomial function in Equation (4), elaborated with the technique of partial least square, fits the data read from technical catalog.

$$T_{sup} = -0.0002T_{out}^3 - 0.016T_{out}^2 - 0.792T_{out} + 39.21 \quad (4)$$

Figure 2 (a) shows the heating curve adopted. On the x-axis, the outside temperature varies in a range between +10 and -30ºC. The residuals between fitted curve and data read from the catalog (Lenhovda et al. 2014) has a maximum magnitude of 0.35ºC. Table 2 lists the panel radiator technical characteristics and an example of panel radiator is shown in Figure 2(c).

Table 2 Characteristics Lenhovda MP50

Height	740 mm	Exponent n	1.2916
Length	2000 mm	Nominal Power	766 W
$T_{sup.}$ / T_{exh} / $T_{air.}$ / ΔT_n	55/45/20/30 ºC	$\overline{\Delta T}$ = $T_{sup.}$ - T_{exh}	10 ºC

The total power from the radiator is calculated according to the following relation:

$$\phi_{tot}(\vartheta) = \phi_n \cdot \left(\frac{\Delta T_{log}(\vartheta)}{\Delta T_n}\right)^n \quad (5)$$

where the $\Delta T_{log}(\vartheta)$ and ΔT_n are accounted as follow:

$$\Delta T_{log}(\vartheta) = \frac{T_{sup.} - T_{exh}}{log\frac{T_{sup.} - T_{air}}{T_{exh} - T_{air.}}} \quad (6)$$

The heat exchanged by radiation is computed by Equation (7) considering only the front surface facing to the indoor space.

$$\phi_{radiative}(\vartheta) = S_{rad.} \cdot \varepsilon \cdot \sigma \cdot \left(\overline{T_m}^4(\vartheta) - \overline{T}_{al}^4(\vartheta)\right) \quad (7)$$

The mean radiant temperature $\overline{T_m}$ of the flow in the panel radiator is calculated as average value between supply and exhaust temperature. The exhaust temperature is calculated by subtracting a ΔT of 10ºC at the supply flow. In the end, the fraction of convective heat is accounted by subtracting from the total power the radiative part. Figure 2(c) shows on the left y-axis the heat exchanged by convection and radiation against the mean radiator temperature. The right y-axis shows the ratio between the radiative and total thermal power provided to the room which varies between 29-38%. In this case, the temperature of the active layer is considered constant at 20ºC. Polynomial curve fits the ratio of radiative/total power from radiator as showed in Figure (2b) and in Equation (8). The residual analysis shows a maximum error of $6\cdot10^{-3}$ºC.

$$ratio = 0.0004 \cdot T_m^2 - 0.0410 \cdot T_m + 1.3098 \quad (8)$$

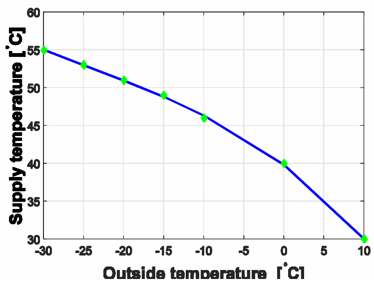

(a)

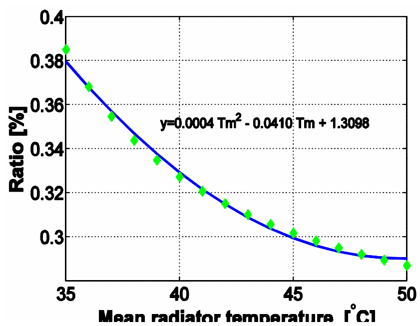

(b)

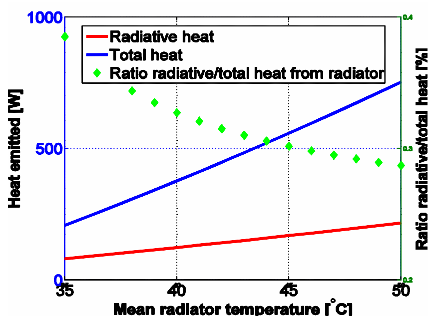

(c)

Figure (2) Panel radiator

Modelling the power from the sun

Solar radiation is responsible for the room overheating when the room control is not fast enough to regulate energy supplied to heating or cooling. The approach used to calculating the loads from the sun is based on Jones method (Jones et al. 1982). The solar model needs as input parameters: longitude, latitude, amount of exposed surface, view factor and transmission factor for glazed surface. The process for calculating the heat gain from sun consists of six steps. First, the declination angle of the earth (δ). . It tells how many degrees the sun is displaced from the plane earth equator. Figure 3(a) shows the earth declination angle depending on the day of the year (n). Equation (8) shows how to calculate it.

$$\delta(\mathrm{n}) = 23{,}45 \cdot \sin\left(360 \cdot \frac{284+n}{365}\right) \tag{8}$$

Second, the altitude of the sun (h). This angle is the inlet of solar radiation in relation to the earth surface at the latitude L_{at}. Equation (9) shows how to calculate this angle.

$$\sin(\mathrm{h}_\vartheta) = \sin(L_{at}) \cdot \sin(\delta_n) + \cos(L_{at}) \cdot \cos(\delta_n) \cdot \cos(\theta_{as}) \tag{9}$$

The sun altitude angle is corrected by the apparent solar time (θ_{as}), which forms a uniform time scale at the specific longitude. Equation (10) calculates the apparent solar time.

$$\theta_{as} = \theta_i + \frac{4 \cdot (L_{zone} - L_i)}{60} + \frac{E}{60} \tag{10}$$

$$\mathrm{E} = 9.87 \cdot \sin(2\mathrm{B}) - 7.53 \cdot \cos(\mathrm{B}) - 1.5 \cdot \sin(\mathrm{B})$$

$$\mathrm{B} = \frac{360}{364}(\mathrm{n} - 81)$$

Daylight saving is included in the apparent solar time. Conventionally, one hour is subtracted at Equation (10) if the day considered falls between the 82nd and 296th day of the year. The apparent solar time is converted in degrees, where each hour corresponds to 15º. Third, the model calculates the angle of azimuth or solar azimuth (a), which is the angle within the horizontal plane measured clockwise from the south. Equation (11) shows the relation.

$$\cos(\mathrm{a}_\vartheta) = \frac{\sin(\mathrm{h}_\vartheta) \cdot \sin(L_i) - \sin(\delta_n)}{\cos(\mathrm{h}_\vartheta) \cdot \cos(L_i)} \tag{11}$$

The fourth step is the angle of incidence (i). It is the angle at which the direct sun radiation strikes on the given surface. Figure 3(b) shows the inclination angle.

$$\cos(\mathrm{i}_\vartheta) = \cos(h_\vartheta) \cdot \cos(a \pm \alpha) \cdot \sin(\gamma) + \sin(h_\vartheta) \cdot \cos(\gamma) \tag{12}$$

The orientation angle of the surface (α) is summed to the azimuth angle (a) if the *ϑ-esima* hour considered is before noon, otherwise it is subtracted. The fifth step consists of calculation of the three component of solar radiation: direct I_D, diffuse I_d and reflected I_{ref}. The direct radiation which strikes on the vertical surface is calculated as follow:

$$I_D = I_{DN} \cdot \cos(\mathrm{i}_\vartheta) \tag{13}$$

I_{DN} is the total irradiance on horizontal surface at the *ϑ-esima* hour of the year. This input parameter is deducted from TRNSYS simulation software. The diffuse radiation is computed as a monthly fraction of the total irradiance on horizontal surface and Table 3 ranks these values. The diffuse radiation is then multiplied for the view factor of the surface (F_{pt}). The surface inclination on the horizontal, the parameter γ gives the view factor.

$$F_{pt} = \frac{1+\cos(\gamma)}{2} \tag{14}$$

Equation (15) expresses the amount of diffuse radiation on the given surface.

$$I_d = I_{DN} \cdot B \cdot F_{pt} \tag{15}$$

The radiation reflected from the surroundings is considered as percentage of direct and diffuse solar radiation. The reflectivity factor depends primarily on the color of surrounding surfaces of the building. Equation (16) shows how to calculate the radiation reflected from surroundings.

$$I_{ref} = (I_d + I_D) \cdot ref \tag{16}$$

Lastly, the heat load applied inside the air volume is calculated by transferring the heat flux applied on the window surface by the use of transmission coefficients. For simplicity, all the transmission coefficients are assumed with the same value of 0.6.

Equation (17) shows the heat gained from the window applied to the air volume. Each part is integrated on the amount of surface heated by the irradiance component.

$$\phi_{sun} = \tau_D \cdot I_D \cdot A_{wi} + \tau_d \cdot I_d \cdot A_{wi} + \tau_{ref} \cdot I_{ref} \cdot A_{wi} \qquad (17)$$

The model divides evenly the total heat gained from the sun between convective and radiative gains. Regarding the building envelope, the total sun radiation (I_{tot}) heats up the external surface determining (T_{sol}) and reducing the heat transfer through the envelope. No heat is gained in the air volume from the envelope.

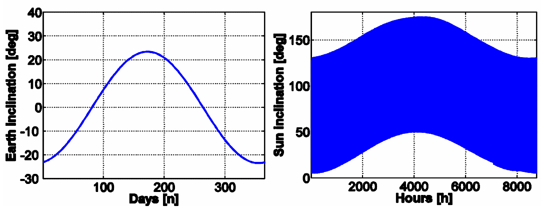

(a) (b)

Figure 3(a) earth inclination 3(b) sun inclination

Table 3 Monthly fraction for diffuse radiation (B)

January	0.058	July	0.136
February	0.060	August	0.122
March	0.071	September	0.092
April	0.097	October	0.073
May	0.121	November	0.063
June	0.134	December	0.057

CONTROL STRATEGY

TRV is the local control of the panel radiator. TRV regulates the amount of heat flow delivered to the panel radiator according to the control strategy adopted. The general control strategy limits the panel radiator to work according to the comfort temperature of occupants. The radiator stops to work when the temperature of indoor air rises over the upper limit of the proportional band. Conversely, the radiator heats the room at the maximum power when the room temperature is below the lower value of the proportional band. Instead, when the room temperature lays in the throttling range, the controller adjusts the thermal power according to the control strategy adopted. Figure 4 shows the proportional band.

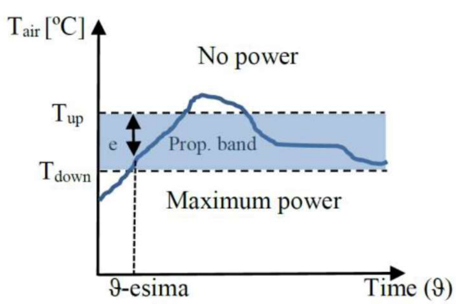

Figure (4): Proportional band

The control strategy consists of applying the three controller P, PI and PID one at a time when the temperature falls in the throttling range. All type of controllers calculate the error (e) between the upper value of the proportional band, set up at 22.5ºC and the *ϑ-esima* value of indoor temperature. This error is then multiplied by the controller gain (K) and in this case we obtain the proportional control P. For PI, the controller calculates the integral time (ϑ_i) considering the past errors. Lastly, the PID also calculates the derivative value (ϑ_{de}) considering the future errors based on the current rate of change of the controlled variable (T_{air}). The tuning of control parameters is performed according to the heuristic theory of Nicholas-Ziegler for close loop. This method tunes the control parameter (K, ϑ_i, ϑ_{de}) by extrapolating them from the step response test. The test consists of exciting the room with an input parameter. In this case the input parameter is the maximum energy available from the panel radiator. The temperature of supply flow to the panel is set up at 55ºC, the outside temperature is constant at 0ºC, solar radiation, internal loads and ventilation are off during the experiment. Figure 5 shows the response of indoor temperature at the input step of energy. The indoor temperature rises till the asymptotic value of 35.02ºC. At the beginning of the test is possible to notice a delay for heating up the indoor air due to the air capacitance. From this curve it is possible to extrapolate the thermal time constant of the room and the parameters for tuning the PID control.

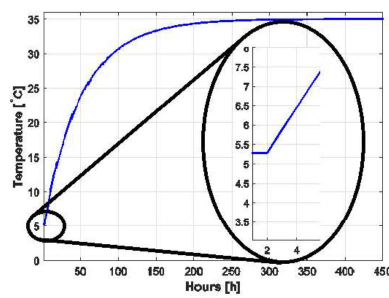

Figure (5): Step response test

The model is written in MATLAB language and it runs on Simulink platform. Simulink is used to connect the core of the model with the control PID.

UNCERTAINTY ANALYSIS

In this work uncertainty analysis identifies which factor gives the larger variation in the model outcomes. Differential sensitivity analysis point tends to know the variation of the output value over the variance of input value. The input value varies locally one at a time keeping all the other factors constant. Such sensitivity approach accounts on finite-difference approximations based on the central differences. This method calculates the partial derivative of the output function with respect of input parameters around their nominal values. The nominal value is the most probable value of each thermal parameter found as previously in this paper. The input parameter selected is subjected to a small perturbation of ±1% around its nominal value. Then, the model reruns passing to the next input parameter. Small perturbations are preferred than large variations since the latter violates the assumption of local linearity. This property is known as the first order effect of sensitivity analysis (Saltelli et al. 1999, MacDonald et al. 2002). The parameters subjected to a small perturbation are: total heat gain, room height, coefficient of heat transfer between air volume and walls, outside temperature, ventilation ratio, envelope surface, windows surface, active layer surface and U values. Positive perturbations of the convective heat gains correspond to negative variations of radiative heat gains and the same procedure is applied for the coefficients of heat transfer by convection and radiation. It should be emphasized that perturbations of room height mean small changes in the volume and therefore in the air capacitance. Variations of window size mean a slightly changing the surface of both envelope and active layer. The program reruns for every next parameter and as a result the uncertainty bands are plotted in Figure 6.

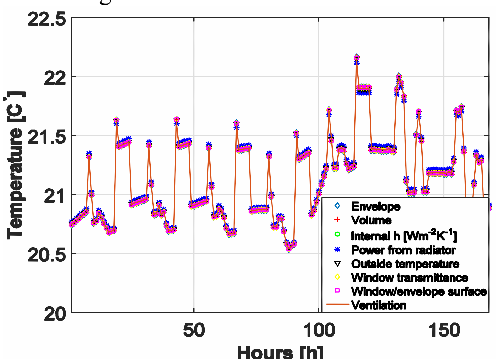

Figure 6: Uncertainty bands

The uncertainty bands are narrow, larger variations are appreciable during winter time when the room needs heating to fulfil the temperature requirements. Figure (7a) shows the variability of indoor temperature with the variation of convective heat. Figure (7b) shows the variability of the indoor temperature with the variation of the outdoor air.

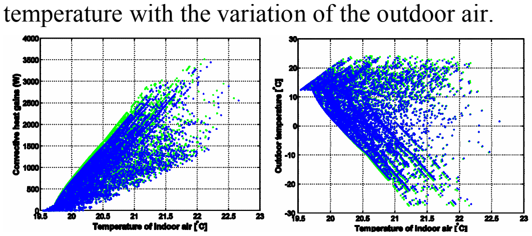

(a) *(b)*

Figure 7(a) Convective heat (b) Outdoor air

Blue spots are the nominal values and the green spots are the perturbed values. The difference between spots is now computed for all the hours in a year with the use of CV RMSE as indicated in Equation 18.

$$CV\ RMSE(\%) = \frac{\sqrt{\sum_{i=1}^{N_p} \frac{(n_\vartheta - s_\vartheta)^2}{N_p}}}{\bar{m}} \tag{18}$$

where n_ϑ and s_ϑ are the nominal and sensitive values of the model outcome at the ϑ-esima hour. N_p is the total number of hours in one year and $\bar{m}$ is the average nominal value of the outcomes calculated for the all year. The problem can be seen from the modeler prospective. The modeler has to assess the most probable value of each thermal parameter, this means that, the modeler needs a tolerance value. This tolerance can be calculated by inverting the problem. It is possible to establish a maximum variation (or maximum value of CV RMSE) at which the model outcomes can be considered still reliable. The maximum variation is fixed with a value of (CV RMSE) of five (Coackney et al. 2014, ASHRAE et al. 2002). The perturbation of each thermal parameter, (before was set up to ±1%) increases at each model round with a step of 1% till the coefficient CV RMSE is fulfilled. Then, the program ends and the last value of the variation represents the tolerance value of the thermal parameter considered. The analysis is repeated for each thermal parameter three times by setting P, PI and PID control. Figure 8 shows the tolerance of each parameter expressed as relative.

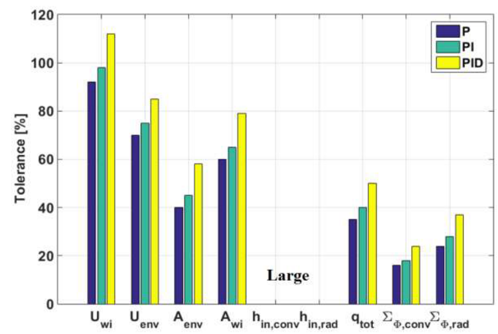

Figure 8: Tolerance of thermal parameters

DISCUSSION AND OUTLOOK

The transmission coefficients (τ), in Equation (17) are affected significantly by the angle of incidence for direct radiation. A better definition of those coefficients would slightly modify the uncertainty bands especially during periods of low heat demand. Therefore, the indoor temperature would oscillates more due to the free sources. This room is located at 63º50' Latitude North where it occurs a period of 6 month of dark. The simulation model is developed around T_{out} and this variable has an impact on several parts of the model. Also, the convective heat is relevant, it directly affects the indoor air. This fact is confirmed by appreciable discrepancies among the sensible values (green spots) and nominal values (blue spots) in Figures (7a, 7b). The uncertainty bands for the indoor air in Figure (6) are narrow. The parameter enables larger variability on the indoor air is the total convective heat. The narrowest of uncertainty bands is also confirmed by similar results obtained by (Clarke et al. 1993, Spitz et al. 2012). The method used for calculating the tolerance, sets the variation with a step increasing of 1%. This fact violates the property of local linearity. This means that, considering Figure (7a), the blue and green spots do not follow anymore a linear correlation. Perhaps, this assumption is weak and a different statistical analysis should be applied for obtaining more precise tolerance. The envelope and window conductance in Figure (8) they enable large errors by switching with more powerful controller. The difference between P and PI is not remarkable, about 5%, but between PI and PID, the difference is more evident (8-9%). This is due to PID that calculates the derivative time (ϑ_{de}) according to the rate of change of controllable variable (T_{air}). This parameter is more sensitive in the variation of indoor temperature than the integral time (ϑ_i). The chart does not show the tolerances of the coefficients of heat transfer by convection and radiation because they are too large. This means that standard values always provide good approximation. A possible model improvement is to use a more detailed room. For instance, to use the commercial software to calculate the radiation between the room internal surfaces. This leads to defining a better indoor temperature. However, in the case studied, the room model set the adiabatic boundary condition for all the walls unless that one facing the outside environment. This assumption helps in the simplification of the radiation between internal surfaces. Another possible improvement is to consider more capacitances in the outside wall. This leads to calculate the heat flow due to the solar radiation striking on the outer surface. Another improvement consists of considering the thermal behaviour of the panel radiator and the TRV. These two components are responsible for how and when the thermal power is delivered into the environment (Tahersima et al. 2010, 2013). In the author´s opinion, this delay can be neglected for the specific case studied, because the discrepancies among the results of different models (commercial and the model used) can be interpreted in relative terms. The tolerance of thermal parameters is a new topic and not well documented. It is always thought, that the tolerance is related to objects with a tangible shape, instead this concept can be irrelevant in the building energy field. This paper is essential for a modeller, as it gives the right idea of what information is more useful for performing a simulation. This concept could also applied it other research fields, for instance in the Energy Certification. The energy auditing does not have all the information when performing evaluation of building thermal characteristics. Furthermore, the control strategy is not always implemented in energy certification software ignoring its functionality. The control is essential because it is the decision maker for managing the energy. As a practical perspective, modellers or energy auditors have ensure the functionality of local control in rooms. This paper could be a benefit for implementing this concept in commercial simulation software or in national building codes. At last, to the knowledge of the author, there is no any type of software available that can model the tolerance beside the nominal value of parameters.

CONCLUSION

The paper shows the tolerance values of thermal parameters addressed to a building simulation model. Three local controls are set up in the simulation. The tolerance value of each thermal parameter is slightly different depending on the type of control set in the room. The local control has a deterministic impact on the model outcome. The PID control reacts faster than PI and P control at the change of indoor temperature. This means that, the indoor air is more stable when a PID control is set up in the room. This concept can be seen from the modeller prospective. The PID control enables the modeller to make larger error (up to 14% than P control and up to 9% than PI) in the evaluation of the thermal parameters. The modeller has to acknowledge every local control in the room and its functionality.

NOMENCLATURE

T = temperature [ºC]
$\emptyset$ = loads [W]
U = conductivity [W m^{-2} K^{-1}]
K = controller gain [Wm^{-2}]
C = thermal capacitance [J ºC^{-1}]
A = surface [m^2]
V = volume [m^3]
c_s = specific heat capacity [Jºkg^{-1} ºC^{-1}]
ρ = density [kg m^{-3}]
e = error [ºC]
h = heat transfer coefficient [Wm^{-2}K^{-2}]
S = radiator surface [m^2]
ε = emissivity
σ = Stefan Boltzmann constant [Wm^{-2}K^{-4}]
ϑ = time [h]
δ = declination angle of the earth [deg]
L_{at} = latitude of the location [deg]
θ_{as} = degree of apparent deviation of the sun from the direction south (noon) at a given time [h]
L_{zone} = latitude of time zone [deg]
L_i = longitude of location of interest [deg]
E = time deviation [min]
γ = pitch angle on horizontal plane [deg]
α = orientation angle of the surface [deg]
β = absorption coefficient [%]
I = sun radiation [Wm^{-2}]
τ = transmittance coefficient [%]
B = monthly fraction [%]
F_{pt} = surface view factor [%]
ref = surface reflectivity factor [%]

subscript and superscript

$_D$ = direct component of radiation
$_{DN}$ = normal component of radiation on horizontal surface
$_d$ = diffuse component of radiation
$_{de}$ = derivative

$_i$ = integral
$_{log}$ = logarithmic temperature
$_m$ = mean
$_n$ = nominal / day /radiator coefficient
$_s$ = simulated
$_{out}$ = outside
$_{sup}$ = supply
$_{exh}$ = exhaust
$_{air}$ = air
$_{al}$ = active layer
$_{env}$ = envelope
$_{wi}$ = window
$_{ach}$ = air change per hour
$_{ext}$ = external
$_r$ = radiative
$_c$ = convective

acronym
HVAC = Heating Ventilation Air Conditioning
TRV = Thermostatic Valve
PID = Proportional Integrated Derivative
CV RMSE = Coefficient of Variation of Mean Root Square

ACKNOWLEDGEMENT

The author wish to thank I Yung Ong for her support and interest in this work.

REFERENCES

Adamson, B., Towards passive houses in cold transfer climates as in Sweden, Department of Architecture and Built Environment Lund University, (2011)

Armstrong, P.R., Leeb, S., Norford, L., Control with building mass thermal response model, ASHRAE Trans. (2006), 1-13

ASHRAE, Guidline 14 2002: Measurament of energy and energy demand savings, American Society of Heating Refrigerating Air-conditioning Engineers

Clarke, J., Strachan, P., Pernot, C., An approach to the calibration of building energy simulation models. ASHRAE Trans., 1993, pp. 990-917

Cengel, Y., Ghajar, A. Heat and mass transfer: Fundamentals and applications, McGrew Hill 4th Edition (2010)

Coakley, D., Raftery, P., Keane, M., A review of methods to match building energy simulation models to measured data, Renewable and sustainable energy reviews, 2014, vol. 37, pp. 123-141

Heoa, Y., Choudhary, R., Augenbroea, G., Calibration of building energy models for retrofit analysis under uncertainty, Energy and Buildings, 2012, vol. 47, pp. 550–560

Jones, W., Handbook of air conditioning and refrigeration, McGrew Hill (1982) 2nd Edition

Lenhovda Värmer, Panel radiator MP-R.O.T., accessed the 10th November 2014

Macdonald, A., Quantifying the effects of uncertainty in building simulation, Department of Mechanical Engineering University of Strathclyde, (2002)

Mata, E., Kalagasidis, A.S., Johnsson, F., Retrofitting measures for energy savings in the Swedish residential building stock-assessing methodology, ASHRAE Trans., (2010), 1-12

Mayers, G. E., Analytical methods in conduction heat transfer, AMCHT Publications Madison, (1998)

Muratori, M., Marano, M., Sioshansi, V., Rizzoni, G., Energy consumption of residential HVAC system: a simple physically-based model, IEEE power and energy society general meeting. San Diego, CA, USA: Institute of Electrical and Electronics Engineers, (2012)

Saltelli, A., Tarantola, S., Chan, K., A quantitative model independent method for global sensitivity analysis of model output, Technometrics 41 (1999), 39-56

Shengwei, W., Chengchu, X. F., Quantitative energy performance assessment methods for existing buildings, Energy and Buildings, 55, (2012)

Silva, A., Ghisi, E., Uncertainty analysis of user behavior and physical parameters in residential building performance simulation, Energy and Buildings, 2014,vol. 76, pp. 381–391

Spitz, C., Mora, L., Wurtz, E., Jay, A., Practical application of uncertainty analysis and sensitivity analysis on an experimental house, Energy and Buildings, vol. 55, 2012, pp. 459–470

Säppanen, O.A., Hausen, A., Hyvrinen, K.Y., Il mastointitekniikka ja sisilmasto, Suomen talotekniikan kehityskeskus Kategoria: Tekniikka, (2004)

Swan, L. G., Ugursal, V.I., K., Modeling of end-use energy consumption in the residential sector: A review of modelling techniques, Renewable and Sustainable Energy Reviews, 13 (2009), 1819-1835

TRNSYS, Multizone building modeling with Type 56 and TRNBuildr, Solar Energy Lab, University of Wisconsin Madison, USA, (2012)

Vitotalk, catalog, Electronic service and viessmannl, Partners in heating technology (August 2003) Issue 5

Xinhua, X., Model based building performance evaluation and diagnosis, Ph.D. Dissertation, Honk Kong University, (2005)

Tahersima, F., Stoustrup, J., Rasmussen, H., An analytical solution for stability-performance dilemma of hydronic radiators Energy and Buildings, 2013, 64, pp. 439-446

Tahersima, F., Stoustrup, J., Rasmussen, H., Nielsem, P. G., Thermal analysis of an HVAC system with TRV controlled Hydronic Radiator, 6th annual IEEE Conference on Automation Science and Engineering, 2010